Available online at www.sciencedirect.com
ScienceDirect
Acta Materialia 56 (2008) 977–984
Acta MATERIALIA
www.elsevier.com/locate/actamat

Determining the interfacial toughness of low-*k* films on Si substrate by wedge indentation: Further studies

Kong Boon Yeap [a], Kaiyang Zeng [a,*], Dongzhi Chi [b]

[a] *Department of Mechanical Engineering, National University of Singapore, 9 Engineering Drive 1, Singapore 117675, Singapore*
[b] *Institute of Materials Research and Engineering, 3 Research Link, Singapore 117602, Singapore*

Received 30 August 2007; received in revised form 24 October 2007; accepted 27 October 2007
Available online 19 December 2007

Abstract

This paper presents further studies to determine the interface toughness of low-*k* films (black diamond (BD) film) using wedge indentation experiments and analysis. In addition, the effects of film thickness on the delamination mode are studied and an analysis methodology is proposed. The curvature of the delamination crack front is measured and compared for the films with different thicknesses, and this information is used to determine the critical buckling stress and the delamination mode: i.e. with or without buckling. For a thinner film with a straight crack front, there is greater likelihood of buckling delamination, while for a thicker film with a curved crack front buckling is less likely. Combining these results with those from a previous study, it is shown that the wedge indentation test is capable of accurately measuring the interface toughness of low-*k* films, and a pop-in event in the load–penetration curve can be used as an early indication of interface crack initiation. It is also found that the resistances to the initiation and propagation of the interfacial cracks for the porous methylsilsesquioxane (MSQ) and non-porous BD films are significantly different; this could be due to the fact that in the porous MSQ film, molecular bridges might provide an additional mechanism to resist interfacial delamination cracks.
© 2007 Acta Materialia Inc. Published by Elsevier Ltd. All rights reserved.

Keywords: Nanoindentation; Dielectrics; Thin films; Interfaces; Toughness

1. Introduction

The continuous scaling of device feature size—the most common means used to improve semiconductor device performance—has eventually reduced the conductive metal line spacing to the nanometer scale. Many new dielectric materials with dielectric constants (k) lower than that of conventional SiO_2 have been introduced in recent years. It is therefore necessary to study the mechanical and functional properties of the new low-k films. The interfacial toughness of the low-k film/substrate is one of the important mechanical properties associated with the application of the various new low-k films.

Various experimental techniques have been developed to study the interface toughness of technologically significant thin film/substrate structures, such as low-k films used in microelectronic devices [1–8]. In a previous work [2], a simple and straightforward indentation testing and analysis method was developed; this method used wedge indentation to determine the interface toughness of a continuous film, without any prior sample preparation procedures. Eliminating the sample preparation steps not only saves time and cost, but also reduces the probability of sample alteration and damage during the preparation processes. It has been shown that this method can determine the interface toughness of methylsilsesquioxane (MSQ) and black diamond (BD) low-k films on Si substrates, and gives results comparable with the literature [2]. In addition, many tests can be done with a small piece of specimen in a relatively short time. For instance, the film delamination only spreads over an area of about 30 μm^2 during the wedge indentation on a 500 nm thick BD film. This work has also shown that the wedge indenter geometry is partic-

* Corresponding author. Tel.: +65 68746627; fax: +65 67791459.
E-mail address: mpezk@nus.edu.sg (K. Zeng).

1359-6454/$30.00 © 2007 Acta Materialia Inc. Published by Elsevier Ltd. All rights reserved.
doi:10.1016/j.actamat.2007.10.051

ularly suitable for characterizing the toughness of the low-k film interface, due to the high crack driving force and the easily observed crack profiles [2].

The details of the analysis and experimental methodology of the wedge indentation test have been reported previously [2]. During that study, it was also found that for a thinner film (BD film 200 nm thick), the front of the delamination crack caused by the wedge indentation was almost straight, whereas for a thicker film (BD film 500 nm thick), the front of the delamination crack was curved. The resulting shape of the delamination cracks, for the 500 nm thick BD film, was considered as an elliptical shape, whereas that for the 200 nm thick BD film was approximated as a rectangular shape. This observation has led to further studies of the effects of the film thickness on the mode and process of the interfacial delamination. In this paper, further studies have been made using the same analysis method described in Ref. [2] and the analysis has been extended in the following aspects: (a) studying the delamination process on 500 nm BD film and its relation with the indentation P–h curves; (b) studying the effects of film thickness on the curvature of interface crack front; (c) introducing and estimating a dimensionless constant, Y, for a film with an intermediate thickness, i.e. a film with the thickness such that the critical buckling stress lies in between that for straight-sided and circular buckling during the wedge indentation tests; and (d) determining the critical buckling stress, σ_c, and interface toughness, G_c, for BD films with different thicknesses based on the measurement of the crack front curvature and delamination area.

2. Experimental methodology

The BD (SiOCH) films investigated here are 100, 300, 500 and 1000 nm thick. Similar to the previous study [2], two nanoindentation systems were used (Nanoindenter XP®, MTS Nano-instruments, MTS Corporation, USA and UMIS-2000H®, CSIRO, Australia). The MTS Nanoindenter XP® with the continuous stiffness measurement (CSM) option was used with a standard Berkovich indenter tip and strain-rate control (0.05 s^{-1}) to determine the elastic modulus and hardness of the BD films. The maximum penetration depths for each of the BD films with different thicknesses were controlled at 50% of the film's thickness.

To study the effects of film thickness on the measured interface toughness, wedge indentation experiments were conducted by using a diamond wedge tip with 90° included angle and a wedge length of 4.055 μm; the wedge tip was mounted on the UMIS-2000H® nanoindenter. A series of wedge indentations were made on each of the BD film samples with different thicknesses. The indentation test consists of three main segments: (a) loading to the predefined maximum load in 20 s, (b) holding at the maximum load for 5 s, and (c) unloading to 30% of the maximum load in 20 s. In addition, to determine the indentation plastic depth, h_p, right before the interface crack kinked to the film surface, 20 indentations were made on each sample with a penetration depth ranging between 30% and 100% of the film thickness. As the value of h_p was determined from the above tests, an additional 20 indentation tests were then performed at the spall-off load, and field-emission scanning electron microscopy (FESEM) (JEOL JSM-5700F, JEOL Corporation, Japan) was used to capture the plane-view images of the delaminated area. After that, imaging software (Scion Image, Scion Corporation, USA) was used to map and calculate the exact area of the delamination. In addition, to determine the critical load for interface crack initiation, a focused ion beam (FIB) (Quanta 200 3D, FEI Company, USA) was used to make cross-sectional cuts at the middle of the wedge indentation impression. Using the plane and cross-sectional views from FESEM and FIB images, the relationship between the interface crack initiation and propagation processes and the nanoindentation load–penetration (P–h) curve was established for the BD/Si system. At least five indentations were cut on each specimen using the FIB technique. Only the results for the 500 nm BD film are presented in this paper, as the correlations for the other BD films are very similar.

3. Results and discussion

3.1. Correlation between P–h curves and crack initiation and propagation

Similar to the case of wedge indentation on MSQ film [2], we will describe correlation studies for the BD films to establish a clear relationship between the nanoindentation P–h curve and the interfacial crack initiation and propagation processes; as the BD film is a non-porous film, the crack initiation and propagation processes could differ from that of the porous MSQ film. For this study, nanoindentations were made with increasing load from 7 to 10 mN using a 90° wedge tip. The correlations of the MSQ and BD films were then compared and the differences discussed.

There are some similarities but also significant differences between the correlations for the MSQ film and the BD film. Fig. 1 shows the nanoindentation P–h curves for 500 nm BD film. It is found that, similar to that observed for MSQ film [2], there is a significant pop-in event in the P–h curve, i.e. an abrupt increase in penetration depth, when indentation depth was about 50% of the film thickness. The actual critical load for interface crack initiation is slightly higher than the pop-in load. The pop-in during wedge indentation on BD films is, however, much pronounced compared to that on MSQ films. Furthermore, FESEM plane-view imaging, and FIB sectioning and imaging were performed on the indentation impressions to relate the delamination processes and the characteristics of the P–h curves. Similar to the findings for the MSQ film, before the pop-in event (7 mN), there is no observable crack on the film surface (Fig. 2a), and as the pop-in occurs (8.5 mN), central and corner cracks can be

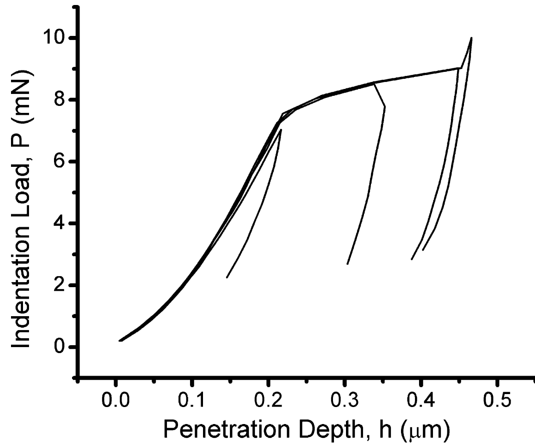

Fig. 1. Load–penetration depth (P–h) curves for 500 nm BD film with maximum indentation load varying from 7 to 10 mN.

clearly seen in the film (Fig. 2b); this suggests that the pop-in in the indentation P–h curve is associated with the central and corner cracks. Further increasing the indentation load to that above the pop-in event (10 mN) will cause film spallation (Fig. 2c). In addition, FIB sectioning at the middle of wedge indentation impression right before the completion of pop-in (9 mN) does not show any interface crack, but the central crack has obviously reached the BD/Si interface (Fig. 2d). Therefore, it can be concluded that the interface crack has been formed, propagated and kinked to the film surface instantaneously at the critical indentation load slightly above the pop-in load (∼10 mN), preventing any observation of the interface fracture process by the FIB sectioning and imaging method. This sequence of interfacial crack initiation and propagation processes is significantly different from that observed in the MSQ film [2]. During the wedge indentation on the porous MSQ film, the interfacial crack is initiated at a lower load (3 mN), then propagates slowly with increasing load and finally kinks to the film surface at a much greater load (9 mN) [2]. In other words, there is a visible crack-propagation process (under FIB sectioning) before the MSQ film spalls off from the surface around the indent. However, for the BD film, the central and corner cracks on the surface during indentation could propagate further without increasing the indentation load as compared to that of the MSQ film.

These differences in the crack initiation and propagation processes between BD and MSQ films are currently under further investigation. One possible explanation could be

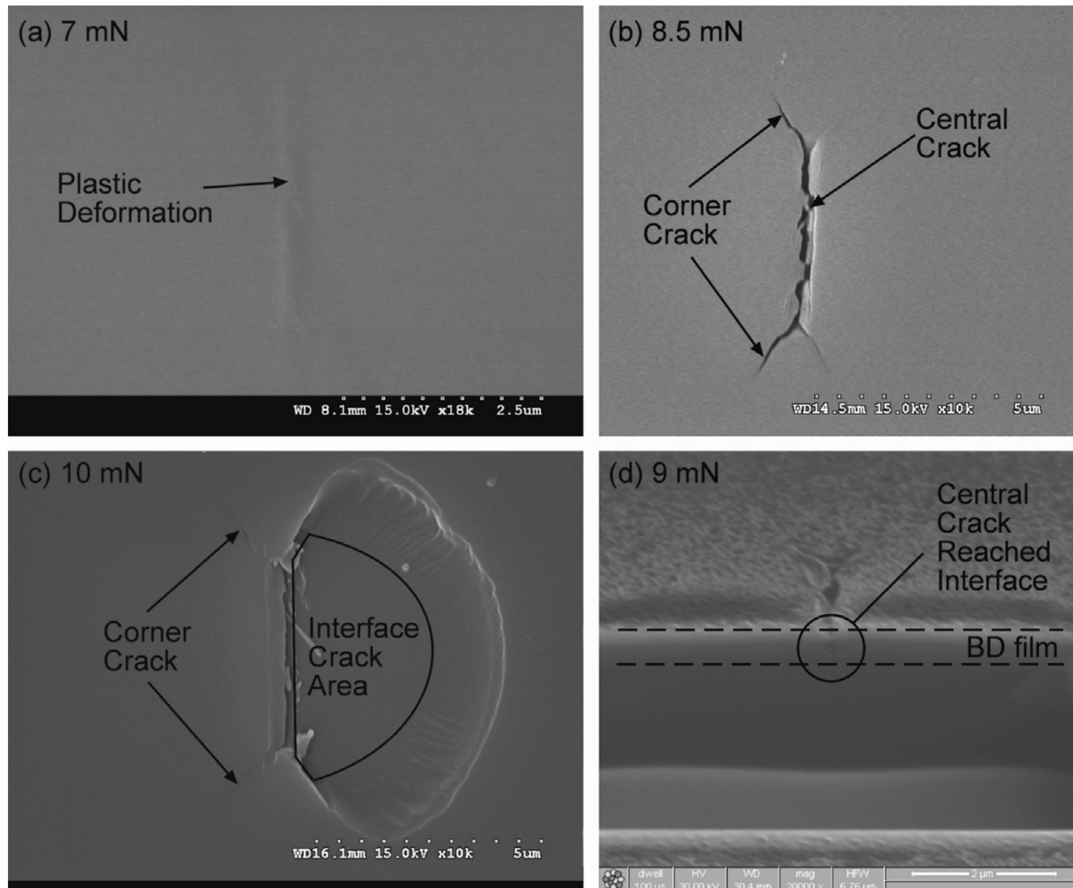

Fig. 2. FESEM plane-view images of 500 nm BD film with maximum indentation loads of (a) 7 mN: only plastic deformation; (b) 8.5 mN: film corner and central crack; (c) 10 mN: complete spall off; and (d) FIB cross-sectional view image of the 500 nm BD film with a maximum load at 9 mN showing no interface crack, but the central crack has reached to the interface.

the different chemical bonding and structures of the films due to their different fabrication methods [7,9]. The BD film was deposited by using a plasma-enhanced chemical vapor deposition (PECVD) technique without creation of pores inside the film, whereas the MSQ film was deposited by using a spin-coating technique and the pores created by removal of porogens added to the matrix. As reported by Maidenberg et al. [9], porogen remnants within the pores of MSQ film might generate molecular bridgings behind the crack tip, and hence a greater driving force will be needed to stretch and break these bridgings to propagate the cracks further. It is possible that due to the energy dissipation provided by stretching of molecular bridgings, further increases of indentation load (from 3 to 9 mN) are required for film and interface crack propagation in the MSQ/Si system. For the BD/Si system, however, both the film and interface cracks are initiated and propagated instantaneously at approximately the same load (7.5–9 mN for film crack and ∼10 mN for interface crack), which suggests the lack of energy dissipation mechanisms that can slow down the crack-propagation process. This will be studied in more detail in the future.

3.2. Elastic modulus of the films

The film's elastic modulus needs to be known in order to determine the interface toughness. As in the previous study [2], the elastic moduli of the BD films were determined by using an MTS Nanoindenter XP with the CSM option. In order to know the substrate effect on the film elastic modulus, the S^2–P analysis method proposed by Page et al. [11] and Saha and Nix [12] was used. In the S^2–P analysis, it has been shown that the values of the elastic modulus and hardness in the penetration depth range where the stiffness squared over the indentation load, S^2/P, remains constant correspond to the film-only properties. Therefore, the elastic modulus measured in this range can be presumed to be the film elastic modulus, and the results of elastic modulus of the BD films are presented in Table 1. These results are further used to calculate the interface toughness (see Section 3.4).

3.3. Curvature of the interface crack front

In Ref. [2], it was noted that the delamination crack front is a straight shape for 200 nm BD film and a circular shape for 500 nm BD film, respectively. The changes in the delamination crack shape due to the different film thicknesses suggest that the critical buckling stress could be dependent on the film thickness. It is well known that the critical buckling stress for a circular buckle is about 50% higher than that of a straight buckle [10,13,14]; therefore, in order to determine the critical buckling stress for different film thicknesses, the curvature of the delamination crack front has to be measured. After determining the critical buckling stresses for the films with different thicknesses, one can then verify the delamination mode, i.e. with or without buckling, by comparing the critical buckling stress with the indentation-induced stress. If the buckling occurs, this must be taken into consideration during the calculation of interface toughness.

In this work, the following approaches have been used to determine the curvature of the delamination crack front. First, a transparent grid paper is used to obtain the coordination along the front of the delamination crack (by defining the origin of the coordination at the middle of the wedge indentation impression); then commercial software (Origin Pro 7.5) is used to fit the delamination crack front with a ninth-order polynomial function, $f(x)$, as shown in Fig. 3. The curvature of interface crack front, κ, for various thicknesses of BD films can then be determined using Eq. (1) and the function $f(x)$ as

$$\kappa = \frac{f''(x)}{[1+(f'(x))^2]^{3/2}}. \qquad (1)$$

At least five measurements are made for each BD film thickness to determine the curvature of the delamination crack front. The relationship between the curvature of crack front and the film thickness is shown in Fig. 4. This relationship suggests that, for a BD film ⩽100 nm thick, the interface crack front is very straight, and hence the critical buckling stress follows the straight-sided buckling mode, and the plane strain condition is fulfilled (Fig. 5a). In contrast, when the BD film thickness is increased to

Table 1
Elastic modulus for BD films with different thicknesses

Film thickness, t (nm)	100	300	500	1000
Elastic modulus, E (GPa)	14.44 ± 5.35	11.69 ± 5.63	9.15 ± 1.08	9.7 ± 0.39

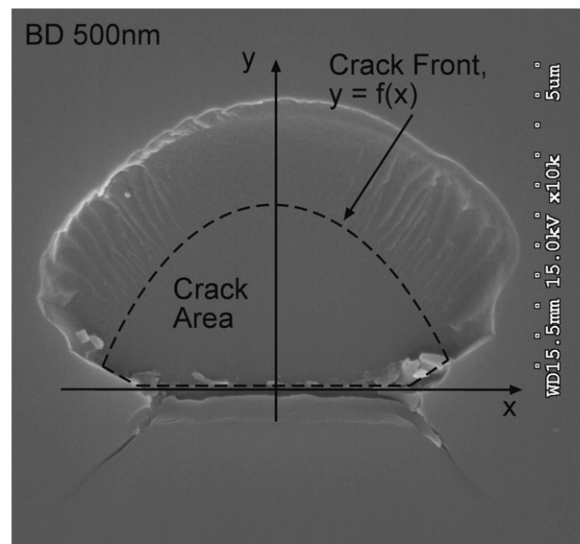

Fig. 3. FESEM plane-view image of delaminated area on 500 nm BD film. A ninth-order polynomial function is fitted to the crack front in order to determine the curvature of the crack front.

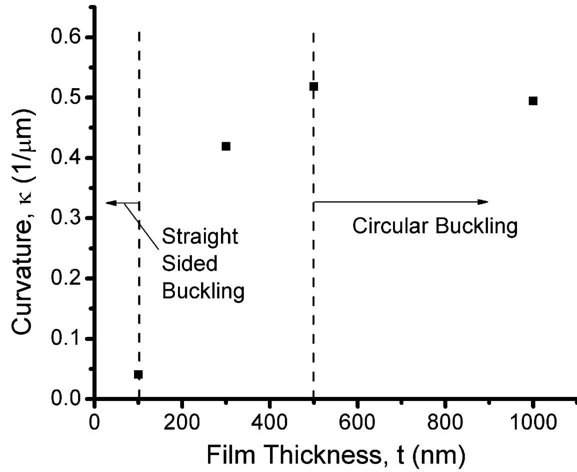

Fig. 4. Curvature of interface crack front determined for BD films with thicknesses ranging from 100 to 1000 nm.

around 500 nm or more, the curvature reaches a plateau at about 0.51 μm^{-1}, and the delamination shape is almost circular, and thus the circular buckling mode should be adopted (Fig. 5c and d). For the 300 nm thick BD film, the crack front is slightly curved (Fig. 5b), and hence the critical buckling stress should be in between that for straight-sided and circular buckling. In order to use the curvature of crack front to estimate the critical buckling stress for intermediate film thickness, such as that for the 300 nm BD film in this case, we propose that the critical buckling stress can be written as follows:

$$\sigma_c = \frac{Y\pi^2}{12}\left(\frac{E_f}{1-\nu_f^2}\right)\left(\frac{t}{a'}\right)^2, \quad (2)$$

where $2a'$ is the crack length in the direction of normal to the wedge indentation impression, and E_f and ν_f are, respectively, Young's modulus and Poisson ratio for the film. A dimensionless constant, Y, is introduced in Eq. (2); this is equal to 1 for straight-sided buckling and 1.488 for circular buckling [2,10]. When estimating the constant Y and critical buckling stress for intermediate thicknesses, we assume that the curvature κ is linearly proportional to the constant Y; if $Y = 1$ is used as a lower bound (κ = 0), and $Y = 1.488$ is used as an upper bound (κ ~ 0.5), then the values of Y for BD films between 100 and 500 nm thick can be estimated and it is found that $Y = 1.39$ for 300 nm film (Table 2). The calculated critical buckling stresses using Eq. (2) are shown in Fig. 6 together with the indentation-induced stresses. As can clearly be seen from Fig. 6, all the BD films ranging from 100 to 1000 nm in thickness show no buckling delamination mode during wedge indentations with the 90° tip, and in all cases, the indentation stresses are lower than the critical buckling stresses for the same film. However, due to the resolution limit of the nanoindentation and imaging equipment (FES-

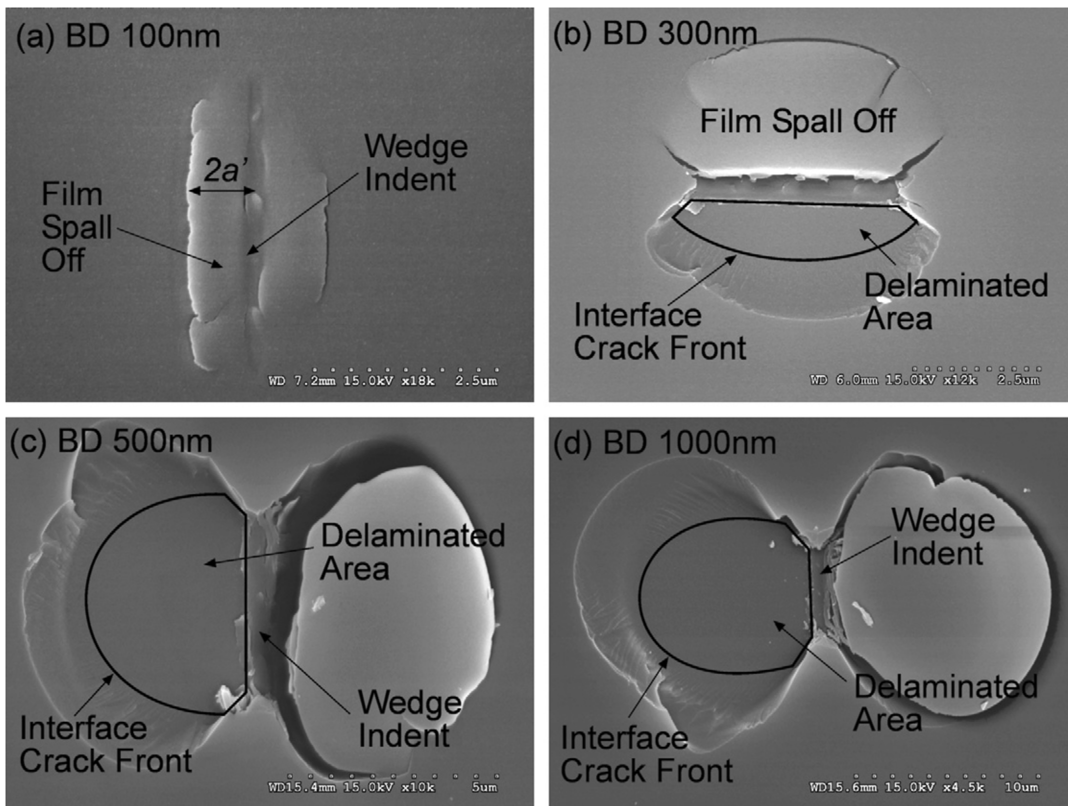

Fig. 5. FESEM plane-view images of the wedge indentation sites and the associated interface crack front on (a) 100 nm BD film: a straight crack front; (b) 300 nm BD film: a slightly curved crack front; (c) 500 nm BD film: a curved crack front, and (d) 1000 nm BD film: almost circular delamination.

Table 2
Curvature of crack front and the dimensionless constant determined for BD films with different thicknesses

	BD film thickness (nm)			
	100	300	500	1000
Curvature of crack front, κ (1/μm)	0.04	0.42	0.52	0.49
Dimensionless constant, Y	1	1.39	1.488	1.488

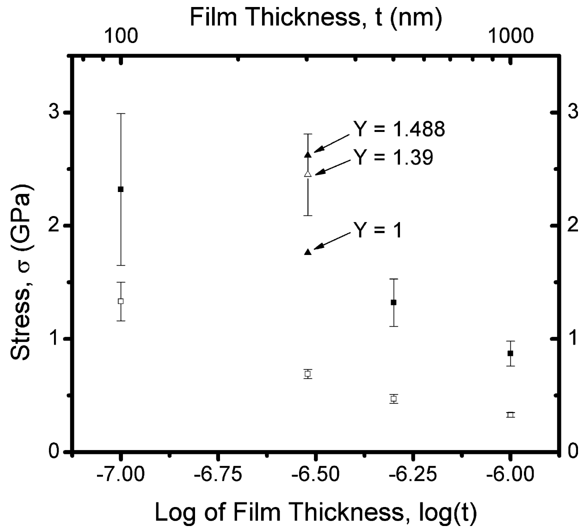

Fig. 6. Comparison between the indentation-induced stress and the critical buckling stress to verify the delamination mode. Open boxes represent the indentation-induced stress calculated from Eq. (3). Closed boxes represent the critical buckling stress calculated using the literature value of $Y = 1$ for 100 nm BD film, and 1.488 for 500 and 1000 nm BD films. For intermediate film thickness, 300 nm BD film, the open triangle represents the critical buckling stress calculated using the approximated value of $Y = 1.39$, while closed triangles represent that calculated by using the upper and lower bounds of Y (1 and 1.488).

EM and FIB), the standard deviations for all the measurements—including the film elastic modulus, crack area and length, and the indentation load and depth—increase as the film thickness decreases. The maximum deviations of the calculated critical buckling stress and indentation-induced stress for the 100 nm thick BD film are quite close to each other (Fig. 6), and might eventually overlap if the film thickness is further decreased to less than 100 nm. When the maximum deviation of critical buckling stress and indentation-induced stress overlap, a mixed delamination mode most likely occurs, i.e. some of the indentations might cause buckling, and some may not. However, we can conclude that for the wedge indentation of thin films, whether the film buckles or not depends on the film thickness: for thicker films, it is most likely that buckling will not occur, while thinner films may buckle during indentation experiments.

3.4. Interface toughness

In this work, a previously reported analysis methodology [2] has been used with some corrections to earlier assumptions. The three simple calculation steps to determine the strain energy release rate, G_c, can be summarized as follows: (a) determine the critical buckling stress and indentation-induced stress by Eqs. (2) and (3), respectively; (b) verify the delamination mode by comparing the critical buckling stress with the indentation-induced stress; and (c) determine G_c for no buckling and for buckling by Eqs. (7a) and (7b), respectively. The indentation-induced stress was found in Ref. [2] to be proportional to the volume ratio, V_0/V_c, and is given as

$$\sigma_0 = E'_f \frac{V_0}{V_c}. \tag{3}$$

The effective modulus, E'_f, is given as

$$E'_f = \frac{E_f}{(1-\nu_f^2)}. \tag{4}$$

The indentation plastic volume, V_0, is given as

$$V_0 = \frac{1}{2} l h_p^2 \tan\phi, \tag{5}$$

where l is the wedge indenter length, h_p is the indentation plastic depth and 2 is the inclusion angle of the wedge indenter tip. The interface crack volume, V_c, is given as

$$V_c = A_c t, \tag{6}$$

where A_c is the interface crack area. It was assumed in the previous study [2] that A_c is elliptical. In this work, accurate mapping and determination of the interface crack area is done by using commercial imaging software (Scion Image). The indentation-induced stress and critical buckling stress can then be compared as shown in Fig. 6. Finally, the interface toughness can be calculated by

$$\Gamma_i = G_c = \frac{(1-\nu_f^2)t\sigma_0^2}{2E_f} \quad \text{(for the no-buckling case)}, \tag{7a}$$

$$\Gamma_i = G_c = \frac{t(1-\nu_f^2)}{2E_f}\left[4\sigma_0\sigma_c - 3(\sigma_c)^2\right] \text{(for the buckling case)}. \tag{7b}$$

The interface toughness of BD films determined from the above procedures is shown in Fig. 7. A minimum of 15 sets of indentation test data were used to calculate G_c. In addition, interface toughness results of MSQ film from the previous study [2] are also included in Fig. 7 for comparison. The two assumptions made in the earlier work about crack area and critical buckling stress are studied further here. Compared to that reported in the previous study [2], the average value and standard deviations of G_c for the BD films with different thicknesses have been reduced, based on a more accurate estimation of the critical buckling stress (as reported in Section 3.1), and the actual crack area determined using imaging software (Scion Image). The average value of interface toughness taken from all the BD films with different thicknesses is 5.39 J m^{-2}, which is smaller than that reported in Ref. [2]. This is due to the fact that in the current work, the

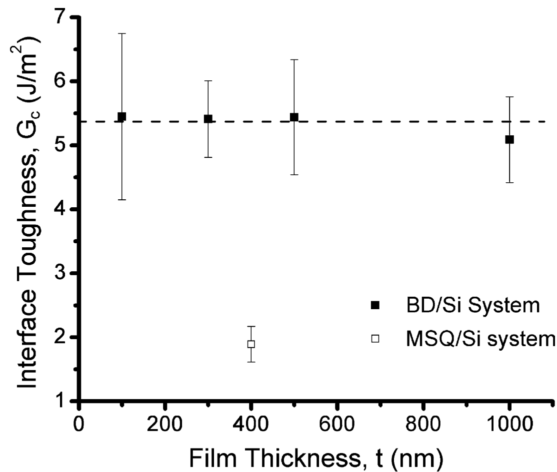

Fig. 7. Interface toughness for BD films with thicknesses ranging from 100 to 1000 nm. The interface toughness for MSQ film measured from the previous study [2] is also included for comparison.

crack front curvature and the areas of the delamination cracks are accurately measured, whereas in the previous work, the crack areas were approximated to a rectangular shape and an elliptical shape, for 200 and 500 nm BD films, respectively. It is also found that the interface toughness for BD films with different thicknesses is a constant, especially for films of intermediate thickness, i.e. from about 150 to 500 nm. This suggests that our assumption about the linear relationship between the curvature and dimensionless constant, Y, should be valid.

The phase angle of steady-state crack propagation at the BD film/Si substrate interface is determined using the method of Hutchinson and Suo [15]. The phase angle is found to be 56° for BD films of different thicknesses, as no buckling occurs in this study; hence the phase angles remain the same for all of the films [2–4].

It is worth noting the differences between the resistance to crack initiation and propagation in the MSQ and BD films. In general, the strain energy release rate, G_c, is composed of two main parts: (a) surface energy, related to the film or interface bonding strength in front of the crack tip; and (b) the plastic energy dissipation behind the crack tip [9]. The MSQ film has a porosity of approximately 30%, and hence the surface energy contribution could be very low and the major toughening mechanisms dependent on the plastic energy dissipation behind the crack tip. As we have discussed above, this plastic energy dissipation could result from the molecular bridgings of the remaining porogens behind the crack tip. On the other hand, the surface energy for the BD film is definitely greater than that for MSQ film due to the dense structure, but the plastic energy dissipated for BD film might be lower than that for MSQ film. These two energy terms might contribute differently to the crack initiation and propagation processes in the two films. The indentation load for crack initiation in the MSQ film (which has a porosity of about 30%) is much lower than that for the BD film, which has a dense structure (3 mN for MSQ film and ~10 mN for BD film). On the other hand, the indentation load needs to be significantly increased (from 3 to 9 mN) to go from crack propagation to film spallation in the MSQ film, whereas for the BD film, the indentation loads for propagation and spallation are very similar (~10 mN). This difference suggests, as we have discussed in the previous section, that there may be plastic energy dissipation during crack-propagation process in the MSQ/Si system, which therefore requires increasing indentation load, whereas for the BD/Si system the interface crack propagates instantaneously right after the initiation process, so that plastic energy dissipation is much less likely. Even though the MSQ/Si system used in our study might have much greater plastic energy dissipation as compared to the BD/Si system, the interface fracture toughness for the MSQ/Si system was found to be lower than that for the BD/Si system (Fig. 7). This is most probably due to the fact that plastic energy dissipation in the MSQ/Si system is not sufficiently greater than the difference in the surface energy or fracture strength between the two systems. Therefore, to further improve the interface toughness of the MSQ/Si system, the chemistry of porogen and matrix materials should be tailored in such a way that large amounts of molecular bridgings can be formed behind the crack tip [9]. For example, Maidenberg et al. [9] have demonstrated that the interfacial fracture toughness of highly porous MSQ films could be increased as the result of the formation of molecular bridgings, and fracture toughnesses of greater than 30 J m^{-2} were obtained.

4. Summary and conclusions

In this work, the interfacial delamination of a BD film from a Si substrate has been studied. It is found that the pop-in event in the indentation P–h curve is related to film cracking, and the interface delamination crack is initiated at an indentation load slightly greater than the pop-in load. These findings are similar to the case of MSQ film. However, it is also found that, unlike the MSQ film/Si system, film and interface cracking for the BD films occurs instantaneously at approximately the same indentation load, which may be explained by the absence of plastic energy dissipation process behind the crack tip in the BD films. The formation of pores within MSQ films results in a reduction in the surface energy, but the plastic energy dissipation term could be increased by the formation of molecular bridging behind the crack tip. However, the MSQ/Si system used in our study may not have a sufficient amount of molecular bridging to compensate for the reduction in interface toughness due to the lower surface energy as compared to the dense BD film. Therefore, the interface toughness measured for the BD/Si system is greater.

The effects of film thickness on the interface delamination processes during the wedge indentation test were also studied in this work. The curvature of the interface crack front for BD films 100, 300, 500 and 1000 nm thick was measured, and a dimensionless constant, Y, introduced in

order to correlate the critical buckling stress with the curvature of the crack front for intermediate film thickness. By comparing the indentation-induced stress and the critical buckling stress, it is found that as the film thickness decreases, a mixed mode delamination may occur. Furthermore, the values of the interface toughness, G_c, have been found to be very consistent for the films with different thicknesses, and the accuracy of determining the interface toughness is improved by precise mapping of the delamination crack area. This work further confirms the validity and usefulness of the methodology developed in our previous study [2] of determining the interface toughness via the wedge indentation technique.

Acknowledgments

The authors would like to thank Ms. L. Shen at the Institute of Materials Research and Engineering (Singapore) for help with the nanoindentation experiments. Thanks to Mr. V.N. Sekhar at Institute of Microelectronics (Singapore) for providing the BD film samples with different thicknesses. This work is supported by National University of Singapore under Academic Research Funds (R265-000-190-112 and R265-000-190-133).

References

[1] Atrash F, Sherman D. J Appl Phys 2006;100:103510.
[2] Yeap KB, Zeng KY, Jiang HY, Shen L, Chi DZ. J Appl Phys 2007;101:123531.
[3] de Boer MP, Gerberich WW. Acta Mater 1996;44:3169.
[4] de Boer MP, Gerberich WW. Acta Mater 1996;44:3177.
[5] Marshall DB, Evans AG. J Appl Phys 1984;56:2632.
[6] Schulze M, Nix WD. Int J Solids Struct 2000;37:1045.
[7] Guyer EP, Patz M, Dauskardt RH. J Mater Res 2006;21:882.
[8] Sanchez JM, El-Mansy S, Sun B, Scherban T, Fang N, Pantuso D, et al. Acta Mater 1999;47:4405.
[9] Maidenberg DH, Volksen W, Miller RD, Dauskardt RH. Nat Mater 2004;3:464.
[10] Moon MW, Jensen HM, Hutchinson JW, Oh KH, Evans AG. J Mech Phys Solids 2002;50:2355.
[11] Page TF, Pharr GM, Hay JC, Oliver WC, Lucas BN, Herbert E, et al. In: Baker SP, Burnham N, Gerberich WW, Moody N, editors. Fundamentals of nanoindentation and nanotribology. Mats Res Soc Symp Proc, 522. Warrendale (PA): TMS; 1998. p. 55–64.
[12] Saha R, Nix WD. Acta Mater 2000;50:23.
[13] Thouless MD, Hutchinson JW, Liniger EG. Acta Metall Mater 1992;40:2639.
[14] Hutchinson JW, Thouless MD, Liniger EG. Acta Metall Mater 1992;40:295.
[15] Hutchinson JW, Suo Z. In: Hutchinson JW, Hu TY, editors. Advances in applied mechanics. New York: Academic Press; 1992. p. 63.